Selected Papers

Electroconductive π-Junction Au Nanoparticles

Masayuki Kanehara,*[1] Jun Takeya,[2] Takafumi Uemura,[2] Hideyuki Murata,[3] Kazuo Takimiya,[4] Hikaru Sekine,[5,6] and Toshiharu Teranishi[5,6,7]

[1]Research Core for Interdisciplinary Sciences, Okayama University, 3-1-1 Tsushimanaka, Okayama 700-8530

[2]Department of Chemistry, Graduate School of Science, Osaka University, 1-1 Machikaneyama, Toyonaka, Osaka 560-0043

[3]School of Materials Science, Japan Advanced Institute of Science and Technology (JAIST), 1-1 Asahidai, Nomi, Ishikawa 923-1292

[4]Department of Applied Chemistry, Graduate School of Engineering, Hiroshima University, Higashi-Hiroshima, Hiroshima 739-8527

[5]Department of Chemistry, Graduate School of Pure and Applied Sciences, University of Tsukuba, 1-1-1 Tennodai, Tsukuba, Ibaraki 305-8571

[6]CREST, Japan Science and Technology Agency, Yokohama, Kanagawa 226-8503

[7]Institute for Chemical Research, Kyoto University, Gokasho, Uji, Kyoto 611-0011

Received April 3, 2012; E-mail: kaneha-m@cc.okayama-u.ac.jp

The fabrication of printed electronic circuits using solution-based electroconductive materials at low temperature is essential for the realization of modern printed electronics including transistors, photovoltaic cells, and light-emitting devices. Despite the progress in the field of semiconductor solution materials, reliable electrodes are always fabricated by a vacuum deposition process resulting in only partially solution-processed devices. In this paper, we show that planar phthalocyanine-conjugated Au nanoparticles (NPs) significantly improve the interparticle-carrier-transport properties. The deposition of a solution of the Au NPs under ambient conditions results in an electroconductive metallic thin film without further post-treatment. Maximum conductivity reaches $>6600\,S\,cm^{-1}$ and the conductivity remains unchanged for at least 1 year under ambient conditions. The all-solution-processed organic field-effect transistor (OFET) fabricated under ambient conditions exhibits mobility values as high as $2\,cm^2\,V^{-1}\,s^{-1}$, the value of which is comparable to OFET devices having vacuum-deposited Au electrodes.

Electrodes are necessary in all types of electric devices such as transistors, photovoltaic cells, and light-emitting devices. These devices are commonly fabricated by employing expensive vacuum deposition processes. A promising alternative that is cheaper and faster for fabricating devices is wet printing using material from specially designed solutions.[1] Many examples of solution processes for transistors,[2–10] photovoltaic cells,[11] and light-emitting devices[12] have been reported. However, in order to achieve high efficiency and reliable devices, vacuum-processed metals and conductive metal oxide electrodes must be used, thereby producing only partially solution-processed devices. To realize the fabrication of all-solution-processed devices, electrodes must be fabricated at relatively low temperatures from a solution, and the resultant electrode must fulfill three requirements: they must have (1) good contacts, i.e., low resistance at the semiconductor–electrode interface, (2) high electroconductivity, and (3) high oxidation stability. In this study, we report that the Au nanoparticles (NPs) possessing orbital hybridization between the Au core and relatively large aromatic molecules meet these three requirements, and consequently, produce reliable electrodes that are comparable to vacuum-deposited Au electrodes.

For the fabrication of NP-based electrodes under ambient conditions, surface ligands of inorganic NPs must meet two requirements: they must (1) adhere firmly to the NP surface for colloidal stabilization and (2) provide stable and facile carrier transport between NPs. We found that orbital hybridization between π orbitals of aromatic molecules and inorganic orbitals of the Au NPs improves the interparticle-carrier transport. The molecular orbital structure of aromatic compounds is altered when the π-conjugated plane of aromatic compounds closely bonds while parallel to the metal surface,[13–15] and this interaction is referred to as a π-junction interaction. We propose a generalized approach for the efficient interparticle-carrier transport between inorganic NPs using large aromatic phthalocyanine (H_2pc) derivatives as ligands. A planar π-conjugated organic H_2pc ligand is capable of achieving a strong π-junction interaction with minimal interparticle-steric

Published on the web August 21, 2012; doi:10.1246/bcsj.20120103

repulsion. In addition, H_2pc derivatives (including porphyrins) are known to coordinate with various types of metal atoms, including Au(0) atoms on Au NPs.[15] Therefore, H_2pc derivatives are promising candidates as π-junction ligands.

Results and Discussion

Syntheses and Properties of Au NPs. We synthesized two H_2pc derivatives, 2,3,9,10,16,17,23,24-octakis[2-(dimethylamino)ethylthio]phthalocyanine (OTAP) and 2,3,11,12,20,21,29,30-octakis[2-(dimethylamino)ethylthio]naphthalocyanine (OTAN). Eight substituted thioether groups elevate the highest occupied molecular orbital (HOMO) level of the ligands to provide the H_2pc ring with the ability to coordinate with Au NPs. Terminal dimethylamino groups cause H_2pc-coordinated Au NPs to dissolve in aqueous solution under acidic conditions. First, we synthesized OTAP and OTAN in two steps from their corresponding halogenated phthalonitrile derivatives. Then, we easily synthesized OTAP- and OTAN-protected Au (OTAP–Au and OTAN–Au) NPs by a ligand-exchange reaction using conventional citrate-capped Au NPs having a diameter of 14.3 ± 2.2 nm[16,17] (For details regarding these syntheses, see the Supporting Information). The synthesized NPs showed good solubility in water under acidic conditions and no solubility under basic conditions, which indicate a successful ligand exchange.

Figure 1 shows images of OTAP–Au and OTAN–Au NPs, with sizes of 14.3 ± 2.3 and 14.4 ± 2.3 nm, respectively. The sizes of Au NPs remained unchanged during ligand exchange. The completion of ligand exchange was confirmed by solubility behavior, laser Raman spectroscopy, and wavelength-dispersive X-ray spectroscopy (WDS). In particular, while the seed citrate-capped Au NPs show no obvious Raman peak from 600 to 1600 cm^{-1}, OTAP–Au and OTAN–Au NPs show distinct peaks that are assigned to the H_2pc ring. These peaks are in good agreement with those observed in Raman spectra of OTAP and OTAN (Figure S1). The Au/sulfur atomic ratios for OTAP and OTAN are 37.8 and 49.8, respectively, as determined by WDS. Assuming that the occupied areas of the molecules of OTAP and OTAN are 2.25 and 2.89 nm^2, respectively, 290 and 230 molecules of OTAP and OTAN, respectively, can densely protect a 14.4-nm Au NP in a face-coordination fashion (Figure 1d). Thus, the Au NP is covered by 260 and 220 molecules of OTAP and OTAN, respectively, which is in good agreement with the calculated number of H_2pc molecules on an Au NP.

Figures 2a and 2b show UV–vis spectra of aqueous solutions of OTAP and OTAN ligands and those of OTAP–Au and OTAN–Au NPs, respectively. The peak positions of OTAP and OTAN Q bands are 664 and 734 nm, respectively. The relatively narrower HOMO–lowest unoccupied molecular orbital (LUMO) energy gap for OTAN results in a red-shifted Q band. Upon coordination with Au NPs, the OTAP Q band decreases significantly, and the OTAN Q band essentially disappears. These drastic spectral changes clearly show the strong π-junction interaction between H_2pcs and Au NPs.[15] This interaction leads to hybridization between the π orbital of the H_2pc and the orbital of Au NPs. As a result, the π orbital of the H_2pc becomes metallic in nature and its continuous band-like nature broadens the UV–vis spectra of Au NPs. The

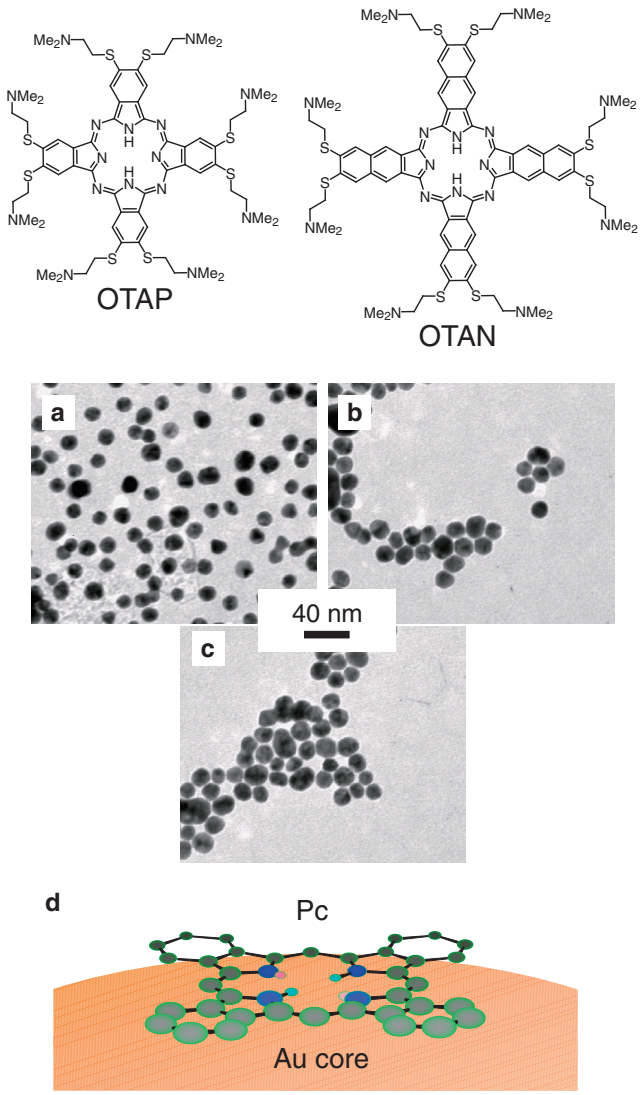

Figure 1. Chemical structures of OTAP and OTAN ligands. TEM images of (a) citrate-protected (14.3 ± 2.2 nm), (b) OTAP-protected (14.3 ± 2.3 nm), and (c) OTAN-protected (14.4 ± 2.3 nm) Au NPs (scale bar: 40 nm). (d) Schematic illustration of the face-coordination of π-junction H_2pc–Au NPs.

disappearance of the Q band reflects the metallic nature of the π orbital of H_2pc on Au NPs, and is similar to the spectra of metallic NPs that have broad absorption from the UV to infrared regions.[18] Recently reported density functional theory (DFT) calculations for the organic semiconductor pentacene on an Au substrate gave similar results, suggesting orbital hybridization between pentacene and Au.[14] Figure 2c shows energy level diagrams for OTAP, OTAN, and Au. The HOMO levels for OTAP and OTAN are 5.53 and 5.34 eV, respectively. The relatively large conjugation area for OTAN can increase the HOMO level to be close to the Fermi level of Au NPs, giving rise to relatively strong π-junction interaction and stabilizing the Au NPs.

Figure 3 shows various properties of OTAN–Au NPs and its thin film. We found that an acidic aqueous formic acid solution of OTAP–Au and OTAN–Au NPs could be used as a printable

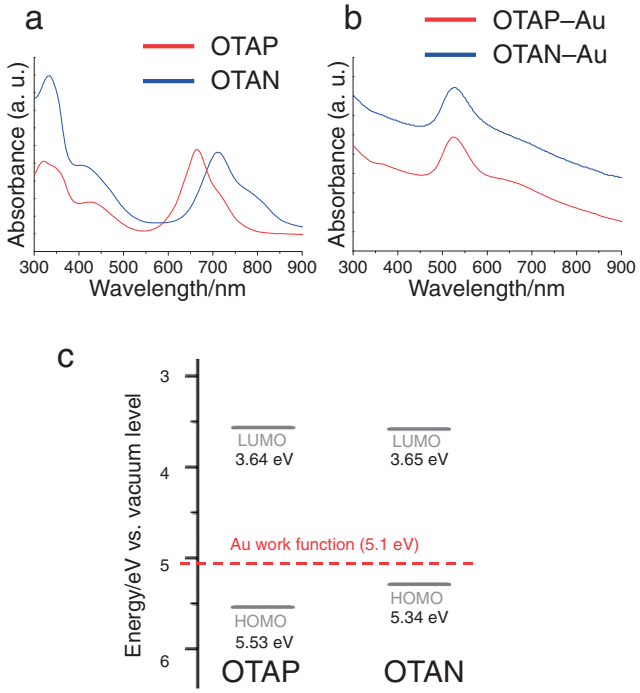

Figure 2. OTAP and OTAN spectra and energy levels: (a) UV–vis spectra of OTAP and OTAN ligands; (b) UV–vis spectra of OTAP–Au and OTAN–Au NPs; (c) energy levels of OTAP and OTAN ligands, showing the Fermi level of Au.

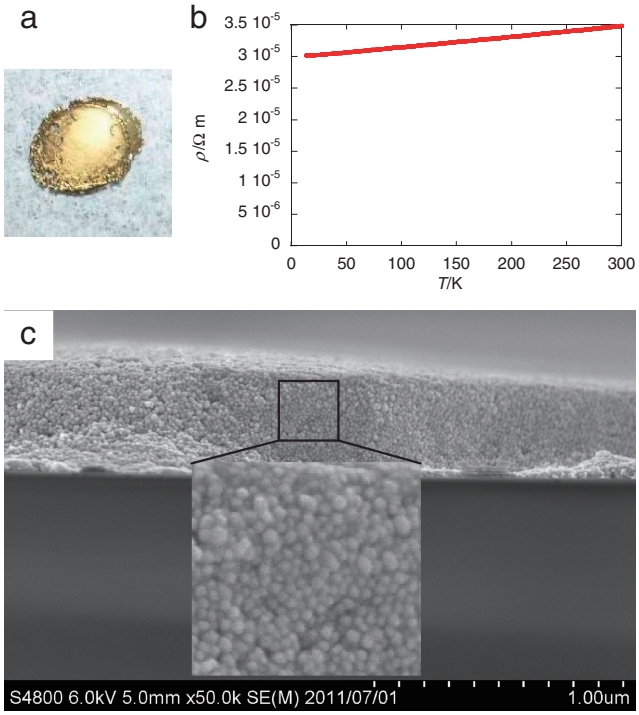

Figure 3. Properties of OTAN–Au NPs and NP thin film: (a) Image of NP thin film dried under ambient conditions; (b) plot of resistivity against temperature for OTAN–Au NP thin film; (c) cross-sectional SEM image of NPs on a glass substrate.

electroconductive material without post-treatment. The purple aqueous solutions of OTAP–Au and OTAN–Au NPs became metallic gold in color after deposition and drying on the substrate under ambient conditions (Figure 3a, see the movie in the Supporting Information). OTAP–Au and OTAN–Au NP thin films, dried at 55 °C for 10 min to remove the remaining solvent, exhibited electric conductivities of 1560 and 6600 S cm^{-1}, respectively. To the best of our knowledge, the highest conductivity reported to date for Au NP thin films was 1000 S cm^{-1}.[19,20] Therefore, OTAN–Au NPs exhibit a conductivity that is more than 5 times higher than that reported. OTAP–Au and OTAN–Au NP thin films are extremely stable, and the electroconductivity of the films remains unchanged for at least two years under ambient conditions. As shown in Figure 2c, the energy gap between HOMO of OTAN and Fermi level of Au is smaller than that of OTAP and Au. This relatively small energy gap leads the strong orbital hybridization between OTAN and Au, which gives greater electric conductivity. The temperature-dependent conductivity of the OTAN–Au NP thin film exhibits a metallic nature, and the resistance decreases with temperature (Figure 3b). The metallic electric junction of the interparticle interface of the OTAN–Au NP thin film was obtained only after drying the OTAN–Au NPs solution under ambient conditions. And the conductivity of the OTAN–Au NP thin film was restricted by the interface between the NPs. A cross-sectional scanning electron microscopy (SEM) image of an OTAN–Au NP thin film fabricated under ambient condition shows the absence of cracks (Figure 3c). Usually, in order to obtain a carrier-transportable NP thin film, annealing at high temperatures (over 150 °C) or washing processes involving the use of chemical reagents such as hydrazine are required to remove insulating ligands, thereby inducing direct interparticle contact.[9,21–23] During such post-treatments, the reduction in the surface-ligand volume always causes cracks on the resultant NP thin film with highly concentrated carrier trap sites.[24] Because OTAP–Au and OTAN–Au NPs do not need such post-treatments, their dried thin films are densely packed structures that are essential for the fabrication of reliable devices.

OFET Device Fabrication. The properties required for electrodes in various types of devices are more stringent than those required for interdevice wiring because an electrode at a semiconductor interface must make good contact.[25] To demonstrate the effectiveness of OTAN–Au NPs, we fabricated all-solution-processed OFETs fabricated under ambient conditions, which are good candidate switching devices for both flexible and printable electronic circuits owing to the development of many solution-processed organic semiconductors.[5] The fabrication of both polymer and small-molecule semiconductors into stable OFETs by near-room-temperature processes have been reported.[6–8,26–28] However, metal electrodes have not yet been fabricated using simple solution techniques. On the other hand, fabrication attempts have resulted in only partially solution-processed devices. We prepared organic semiconductor layers of 2,7-dioctyl[1]benzothieno[3,2-*b*]benzothiophene (C8-BTBT) using a crystallizing technique developed by one of the authors to enable an easy fabrication of large-domain crystalline films on an Si–SiO_2 substrate.[28] We then painted a solution of OTAN–Au NPs on the semiconductor film at room

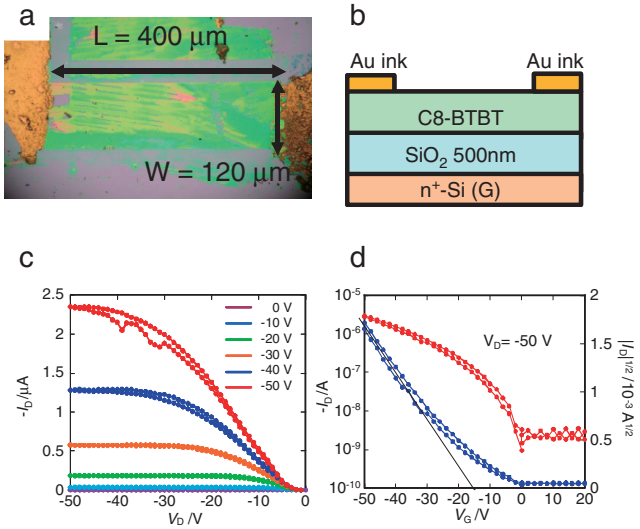

Figure 4. Full solution-fabricated OFET made using a solution-deposited C8-BTBT semiconductor layer coated with OTAN–Au NPs and used for electrodes: (a) Top view; (b) schematic illustration; (c) output characteristics; (d) transfer characteristics.

temperature to construct a top-contact, bottom-gate OFET. Figure 4 shows different views and characteristics of the constructed OFET. The channel length and width are 400 and 120 μm, respectively (Figures 4a and 4b). The typical transistor characteristics demonstrate clear FET performance with mobility values as high as 2 $cm^2 V^{-1} s^{-1}$ (Figures 4c and 4d). This value is comparable to the previously reported value for the mobility of devices having vacuum-deposited Au electrodes, which ranged from 3.5 to 5 $cm^2 V^{-1} s^{-1}$.[28] We note that the structure and the channel dimensions are essentially same for the previously reported solution-crystallized C8-BTBT OFETs as compared with the present devices incorporating the π-junction Au NPs. Therefore, the results indicate general usefulness of painted OTAN–Au NPs that were fabricated using a very simple room-temperature method described here. The mechanism that causes a slightly smaller value of mobility in the present devices is under investigation in order to further increase the transistor performances. It can be suspected that the present paining process results in slightly more resistive metal–semiconductor contacts or that the vapors from the water-based solvent induced shallow hole-trapping levels attached to the surface of the C8-BTBT channels.

Conclusion

We have demonstrated that H_2pc-derivative-protected π-junction Au NPs can be fabricated into electroconductive circuits and electrodes by room-temperature printing. The HOMO level of H_2pc is sufficiently close to the Fermi level of Au, which is a requirement for inducing a strong interorbital interaction between H_2pc and the Au NP core, resulting in good electroconductivity of the deposited Au NP thin film (>6600 S cm^{-1}). An all-solution-processed OFETs fabricated under ambient conditions has a mobility of 2 $cm^2 V^{-1} s^{-1}$. Electroconductive π-junction metal NPs are the only solution materials that can produce high-performance OFETs that are comparable to conventional vacuum-deposited metal electrodes.

Experimental

Syntheses of OTAP– and OTAN–Au NPs. The aqueous citrate-capped Au NPs (1 L, 2 mM as Au atom) were prepared according to the method described by Ji et al.[17] An acidic aqueous formic acid solution of OTAP (20 mg) or OTAN (20 mg) was added to the solution. After stirring at room temperature for 30 min, an excess amount of aqueous trimethylamine was added. The resultant precipitate was centrifuged and washed with water and ethanol to give pure OTAP– and OTAN–Au NPs.

Conductivity Measurement of OTAP– and OTAN–Au NPs. A solution of OTAP–Au NPs was painted at room temperature on a quartz substrate to draw conductive lines. It was then dried at 55 °C for 10 min. The line width and thickness were 1.04 mm and 2.03 μm, respectively, as measured with a surface profilometer (Dektak 3030). Line conductivities were measured using the four-point probe method, where a force current (10 mA) was applied to the line by a pair of outside probes. To measure the resistance uniformity along the gold line, the distance L between the interior terminals was varied. The conductivities measured at three different positions were 1571, 1528, and 1582 S cm^{-1}, with an average conductivity of 1560 S cm^{-1}. Similarly, a solution of OTAN–Au NPs was painted at room temperature on a quartz substrate to draw conductive lines, and then dried at 55 °C for 10 min. The line width and thickness were 1.04 mm and 0.905 μm, respectively. The average conductivity measured at four different positions was 6604 S cm^{-1}, and the maximum conductivity was 7012 S cm^{-1}.

This work was supported by a Grant-in-Aid for Scientific Research on Innovative Areas (No. 23108702, "pi-Space"), Young Scientists (A) (No. 23685028) (M.K.), Special Coordination Funds for Promoting Sciences and Technology (M.K.), and Scientific Research (A) (No. 23245028) (T.T.) from the MEXT, Japan.

Supporting Information

Syntheses of OTAP and OTAN ligands, laser Raman spectra, 4-probe conductivity measurement of OTAP– and OTAN–Au thin film, and the movie of the double speed drying process of OTAN–Au NPs. This material is available free of charge via the Internet at http://www.csj.jp/journals/bcsj/.

References

1 *Solution Processing of Inorganic Materials*, ed. by D. B. Mitzi, Wiley, New York, **2009**.
2 M.-G. Kim, M. G. Kanatzidis, A. Facchetti, T. J. Marks, *Nat. Mater.* **2011**, *10*, 382.
3 J. Rivnay, L. H. Jimison, J. E. Northrup, M. F. Toney, R. Noriega, S. Lu, T. J. Marks, A. Facchetti, A. Salleo, *Nat. Mater.* **2009**, *8*, 952.
4 Y.-Y. Noh, N. Zhao, M. Caironi, H. Sirringhaus, *Nat. Nanotechnol.* **2007**, *2*, 784.
5 H. Sirringhaus, P. J. Brown, R. H. Friend, M. M. Nielsen, K. Bechgaard, B. M. W. Langeveld-Voss, A. J. H. Spiering,

R. A. J. Janssen, E. W. Meijer, P. Herwig, D. M. de Leeuw, *Nature* **1999**, *401*, 685.

6 H. Minemawari, T. Yamada, H. Matsui, J. Tsutsumi, S. Haas, R. Chiba, R. Kumai, T. Hasegawa, *Nature* **2011**, *475*, 364.

7 H. Yan, Z. Chen, Y. Zheng, C. Newman, J. R. Quinn, F. Dötz, M. Kastler, A. Facchetti, *Nature* **2009**, *457*, 679.

8 I. McCulloch, M. Heeney, C. Bailey, K. Genevicius, I. MacDonald, M. Shkunov, D. Sparrowe, S. Tierney, R. Wagner, W. Zhang, M. L. Chabinyc, R. J. Kline, M. D. McGehee, M. F. Toney, *Nat. Mater.* **2006**, *5*, 328.

9 D. V. Talapin, C. B. Murray, *Science* **2005**, *310*, 86.

10 G. Konstantatos, I. Howard, A. Fischer, S. Hoogland, J. Clifford, E. Klem, L. Levina, E. H. Sargent, *Nature* **2006**, *442*, 180.

11 I. Gur, N. A. Fromer, M. L. Geier, A. P. Alivisatos, *Science* **2005**, *310*, 462.

12 J. M. Caruge, J. E. Halpert, V. Wood, V. Bulović, M. G. Bawendi, *Nat. Photonics* **2008**, *2*, 247.

13 G. V. Nazin, X. H. Qiu, W. Ho, *Science* **2003**, *302*, 77.

14 Y. J. Song, K. Lee, S. H. Kim, B.-Y. Choi, J. Yu, Y. Kuk, *Nano Lett.* **2010**, *10*, 996.

15 M. Kanehara, H. Takahashi, T. Teranishi, *Angew. Chem., Int. Ed.* **2008**, *47*, 307.

16 J. Turkevich, P. C. Stevenson, J. Hillier, *Discuss. Faraday Soc.* **1951**, *11*, 55.

17 X. Ji, X. Song, J. Li, Y. Bai, W. Yang, X. Peng, *J. Am. Chem. Soc.* **2007**, *129*, 13939.

18 M. Kanehara, E. Kodzuka, T. Teranishi, *J. Am. Chem. Soc.* **2006**, *128*, 13084.

19 M. V. Kovalenko, M. Scheele, D. V. Talapin, *Science* **2009**, *324*, 1417.

20 M. V. Kovalenko, M. I. Bodnarchuk, J. Zaumseil, J.-S. Lee, D. V. Talapin, *J. Am. Chem. Soc.* **2010**, *132*, 10085.

21 A. Zabet-Khosousi, A.-A. Dhirani, *Chem. Rev.* **2008**, *108*, 4072.

22 D. Wakuda, M. Hatamura, K. Suganuma, *Chem. Phys. Lett.* **2007**, *441*, 305.

23 M. Yamamoto, H. Kakiuchi, Y. Kashiwagi, Y. Yoshida, T. Ohno, M. Nakamoto, *Bull. Chem. Soc. Jpn.* **2010**, *83*, 1386.

24 M. Law, J. M. Luther, Q. Song, B. K. Hughes, C. L. Perkins, A. J. Nozik, *J. Am. Chem. Soc.* **2008**, *130*, 5974.

25 T. Miyadera, T. Minari, K. Tsukagoshi, H. Ito, Y. Aoyagi, *Appl. Phys. Lett.* **2007**, *91*, 013512.

26 J. E. Anthony, J. S. Brooks, D. L. Eaton, S. R. Parkin, *J. Am. Chem. Soc.* **2001**, *123*, 9482.

27 H. Ebata, T. Izawa, E. Miyazaki, K. Takimiya, M. Ikeda, H. Kuwabara, T. Yui, *J. Am. Chem. Soc.* **2007**, *129*, 15732.

28 T. Uemura, Y. Hirose, M. Uno, K. Takimiya, J. Takeya, *Appl. Phys. Express* **2009**, *2*, 111501.